Influence of face reinforcement and shotcrete support on static conditions of deep tunnels: a thermo-chemo-mechanical study

Daniela Boldini,* Roman Lackner,** Herbert A. Mang**

Summary

In the last years, the combination of shotcrete as primary lining and face reinforcement by means of fiber-glass dowels was successfully employed during tunneling in squeezing conditions (e.g., in soft rocks under high overburden stress). In this paper, numerical results obtained from axisymmetric analyses considering the application of the shotcrete lining and the installation of fiber-glass dowels at the tunnel face during the tunnel excavation are presented. The geometric and mechanical characteristics of the support means as well as the time schedule of excavation, shotcreting, and reinforcement stages were selected accordingly to the design and performance of a recently-built Italian tunnel (the Raticosa tunnel). The numerical study focused on the investigation of the behavior of deep tunnels excavated in moderate- to high- squeezing conditions. Accordingly, a viscoplastic material model was chosen for the description of the mechanical behavior of the ground. The behavior of shotcrete was described in the framework of thermo-chemo-mechanics. The obtained results provide insight into the ground-shotcrete interaction, the effect of face reinforcement by means of fiber-glass dowels, and the state of stress in the shotcrete lining. Moreover, the variation of ground properties and the reinforcement density made it possible to evaluate the loading and effectiveness of the employed support means for different geotechnical conditions.

1. Introduction and description of the problem

Large ground deformations in the course of the excavation of deep tunnels in poor geotechnical conditions result in an unacceptable reduction of the tunnel clearance, stability problems, and overstressing of the support elements. These conditions are generally referred to as squeezing conditions. Following the International Society of Rock Mechanics, «Squeezing of rock is the time-dependent large deformation which occurs around the tunnel and is essentially associated with creep caused by exceeding the limiting shear stress. Deformations may terminate during construction or continue over a long period» [ISRM, 1994].

The magnitude and rate of tunnel deformations related to squeezing depend on several factors such as the geological conditions, in situ stress, and groundwater regime as well as the geotechnical properties of the ground and the tunneling technique. The squeezing potential may be related to the ratio between the uniaxial strength of the ground f_c and the in situ stress σ_0. Poor geotechnical conditions result in values of the f_c/σ_0-ratio less than 0.2 and, hence, in severe squeezing conditions.

* Department of Structural and Geotechnical Engineering, University of Rome «La Sapienza», Italy

** Institute for Mechanics of Materials and Structures, Vienna University of Technology, Austria

The consequences of squeezing may be reduced by an appropriate tunneling technique [ISRM, 1994]. Immediate support of the excavated surfaces, e.g., reduces the yielding of the ground around the tunnel, thus limiting the short- and long-term deformations. Recently, the stability of the tunnel face has been recognized as the critical factor for assuring the stability of the tunnel, especially in excavations characterized by tunnel cross-sections exceeding 10 m in diameter [Lunardi, 2000].

Several techniques have been developed to provide face stability during tunneling in squeezing conditions. They include sequential excavation methods (i.e., side-drift method, top heading and benching down excavation method), pre-lining techniques (i.e., mechanical pre-cutting followed by concrete shell cast) and pre-confinement techniques (i.e., pipe roofing, horizontal jet-grouting) as well as ground improvement by means of grouting, freezing, and dewatering. Whereas all these techniques reduce the excavation rate significantly, a novel technique characterized by face reinforcement, by means of fiber-glass dowels, in combination with full-face excavation and immediate shotcreting of the excavated surfaces, provides the possibility of highly-mechanized tunneling using larger equipment as well as the flexibility required in case of variable geotechnical conditions [Schubert *et al.*, 2000]. Although this construction method has been adopted in many countries [Kovari *et al.*, 2000], the available design methods are not satisfactory: they are based

either on the experience of the contractors and consultants involved in the project, or on oversimplified assumptions regarding the reinforcement systems and the shotcrete support.

Analytical expressions and numerical studies dealing with face reinforcement basically confirm the key role of face reinforcement in reducing the tunnel deformations and in assuring face stability. Analytical approaches take advantage of the generally high density of the reinforcement layout, assuming the ground reinforced by dowels to be a homogenized medium [JASSIONESSE *et al.*, 1996; DIAS *et al.*, 1998; WONG *et al.*, 2000]. In order to investigate the effect of face reinforcement on the full stress-strain conditions around the tunnel and on the displacement at the ground surface, numerical analyses were performed [PEILA, 1994; PEILA *et al.*, 1996; YOO & SHIN, 1999; YOO, 2002; NG & LEE, 2002]. The reinforcement by fiber-glass dowels was considered by (i) introducing each dowel into the Finite Element mesh [e.g., PEILA, 1994], (ii) increasing ground cohesion ahead of the tunnel face, or (iii) applying a fictitious pressure at the tunnel face [e.g., PEILA *et al.*, 1996]. Whereas approaches (ii) and (iii) require less computational time, they assume the dowels to be loaded at their limit load [WONG *et al.*, 2000]. In fact, the load-carrying capacity of the dowels is not always fully mobilized, resulting in an overestimation of the effect and, hence, of the increase in safety provided by the dowels.

Similar to the critical length, a critical reinforcement density exists, where at densities higher than the critical density, additional dowels do not increase the reinforcing effect [NG & LEE, 2002]. A possible counter-effect of the reinforcement of the ground ahead of the tunnel face could be the increase in the stress in the primary lining placed during the excavation [PEILA *et al.*, 1996].

The numerical results presented in the scientific literature have been obtained from simplified models by considering dowels ranging over the entire FE mesh, by disregarding the excavation steps associated with the installation of the dowels, by simulating tunnel excavation by one-single excavation step, and, finally, by disregarding the influence of shotcrete behavior.

In order to improve the understanding of the load-carrying behavior of deep tunnels driven by full-face excavation in squeezing ground conditions and supported by the application of a shotcrete lining and by face reinforcement with fiber-glass dowels, 3D axisymmetric analyses of tunnel excavation were performed. The construction steps, including tunnel excavation, shotcrete application, and reinforcement of the tunnel face by fiber-glass dowels, are modeled in detail, following the design and performance of the recently-built Raticosa tunnel (Italy), where the investigated tunnel technique was successfully applied [BOLDINI *et al.*, 2004].

Consideration of thermo-chemo-mechanical couplings in the material model for shotcrete requires the solution of two subsequent analyses. First, the thermo-chemical analysis accounting for the thermally-activated nature of the hydration process of shotcrete is performed. It provides the temperature field in the ground and the temperature field and the hydration extent in the shotcrete lining. This result is used as input for the subsequent mechanical analysis, providing insight into the ground-shotcrete interaction, into the effect of face reinforcement by means of fiber-glass dowels, and into the state of stress in the shotcrete lining. Finally, the influence of the face reinforcement density on tunnel deformations is investigated in different geotechnical conditions by varying the ground cohesion over a wide range of values, representing conditions of moderate- to high- squeezing potential.

The main characteristics of the Raticosa tunnel and the adopted construction scheme will be outlined in the following section. Then, the constitutive models for the ground, the shotcrete, and the fiber-glass dowels are given. After a brief description of the two-step analysis scheme, comprising the solution of the thermo-chemical and the mechanical problem, results obtained for different densities of the face reinforcement and for varying cohesion of the ground will be presented.

2. Raticosa Tunnel, Italy

The high-speed railway line from Bologna to Florence is one of the most important segments of the Milan-Naples high-speed line. It has a strategic function for the whole Italian railway system. The route crosses the Tosco-Emiliano Apennines, a large mountain chain characterized by complex geotechnical conditions.

One of the most challenging situations encountered during the design stage was the crossing of a tectonized clay-shale formation known as «Chaotic Complex». The overburden in this area measures up to 500 m.

2.1. Geological conditions and geotechnical characterization

The Chaotic Complex reached its current position after intensive tectonic events during the Miocene-Pliocene and Plio-Pleistocene. It is mainly composed of a pelitic matrix with dispersed lithic components. The pelitic component consists of scaly clays, characterized by well-packed systems of randomly oriented scales. The clay scales are flaky

Fig. 1 – Raticosa tunnel, Italy: tunnel face supported by a temporary shotcrete shell and fiber-glass dowels.
Fig. 1 – La galleria Raticosa, Italia: fronte di scavo sostenuto da un rivestimento temporaneo in calcestruzzo proiettato e da barre in vetroresina.

shaped ranging in size from a few millimeters to several centimeters. The lithic components include calcareous, marly and arenaceous blocks for a total volume fraction varying between zero and some ten-twenty percent. However, because of the low percentage of the lithic components which are mainly present in the form of disarranged strata and fragments, the mechanical behavior of the Chaotic Complex is governed by the clay-shale matrix.

In the course of the geotechnical characterization of the clay-shale matrix, difficulties and uncertainties, mainly related to the high sensitivity to sampling disturbance and specimen preparation of the pervasively fissured stiff clayey material, were encountered. Details of the geotechnical characterization can be found in BOLDINI *et al.* [2004].

2.2 Design and performance

The design of the tunnel was based on the ADECO-RS approach [LUNARDI & FOCARACCI, 1999]. The distinctive feature of this approach is to highlight the key role of the tunnel face stability for the overall static conditions of the tunnel. Because of the squeezing conditions predicted in the preliminary investigation phase, full-face excavation was combined with face reinforcement by means of fiber-glass dowels (Fig. 1). In addition, a closed primary lining consisting of a shotcrete shell and steel sets, including an arched strut in the invert, was adopted.

The cross-section of the Raticosa tunnel is shown in Figure 2. It is defined by the radii R1, R2, and R3. The geometric characteristics of the cross section are summarized in Table I.

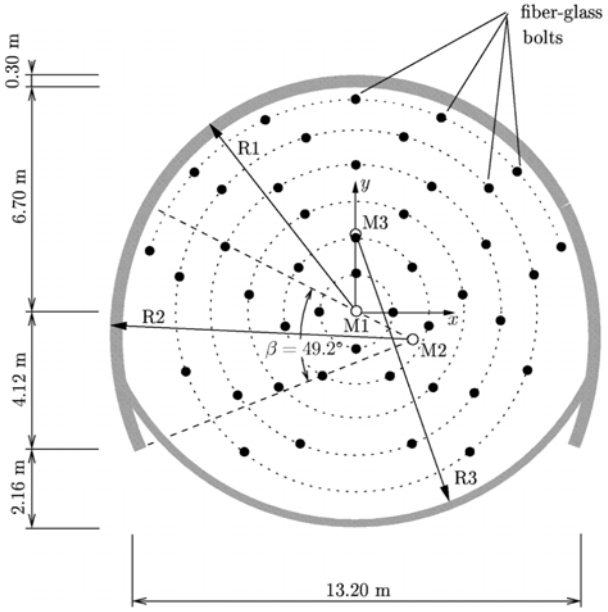

Fig. 2 – Raticosa tunnel, Italy: cross section.
Fig. 2 – La galleria Raticosa, Italia: sezione trasversale.

In the numerical analyses presented here, reference will be made to the construction scheme employed at the Raticosa tunnel during July and August 2000. In these tunnel sections (i.e., from chainage 32+270 to chainage 32+198) the construction scheme was characterized by:

– reinforcement of the tunnel face with 45 fully-grouted fiber-glass dowels every 12.5 m of excavation. The dowels were 24 m long giving an overlap of 11.5 m (see Fig. 3);

Tab. I – Raticosa tunnel, Italy: geometric properties of the cross section.
Tab. I – La galleria Raticosa, Italia: proprietà geometriche della sezione trasversale.

	x [m]	y [m]	R [m]
M1	0.00	0.00	7.00
M2	1.81	-0.75	8.96
M3	0.00	1.23	7.50

Tab. II – Raticosa tunnel, Italy: properties of the primary lining and fiber-glass dowels.
Tab. II – La galleria Raticosa, Italia: proprietà del rivestimento di prima fase e delle barre in vetroresina.

steel arch HEA 300	Fe430
shotcrete	
compressive strength	at 48 hours 13 MPa
(core samples with $h/\phi = 1$)	at 28 days 20 MPa
fiber-glass dowel	
reacting area	8.4 cm^2
tensile strength	900 MPa
Young's modulus	15000 MPa

– closed primary lining consisting of a 30 cm thick shotcrete shell and steel sets (type HEA 300) installed every 1.04 m of tunnel advance);
– support of the tunnel face by a shotcrete shell with a thickness of 10 cm during the installation of the fiber-glass dowels.

The properties of the employed materials are listed in Table II.

The tunnel was driven by full-face excavation in steps of 1.04 m. Figure 4 shows the location of the tunnel face, the invert arch and the final lining for the considered part of the tunnel, driven in July and August 2000. The setting of the dowels took 3 days. During this period of time, the invert arch was installed. The excavation of the tunnel from one face reinforcement to the consecutive face reinforcement, i.e., the excavation of 12.5 m, took approximately 5 days, giving a tunnel excavation rate of 2.5 m/day. On August 7th, the tunnel excavation was stopped for three weeks for the summer holidays.

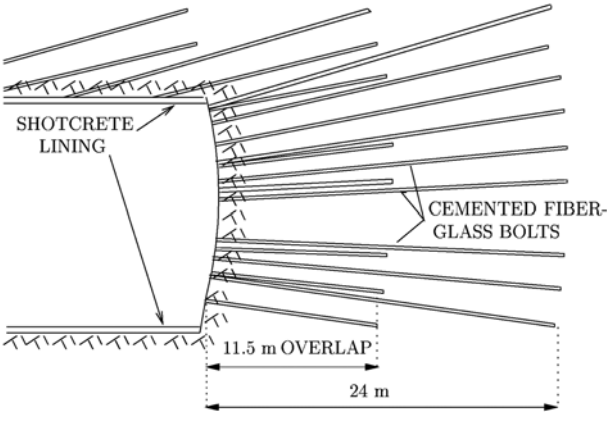

Fig. 3 – Raticosa tunnel, Italy: longitudinal section.
Fig. 3 – La galleria Raticosa, Italia: sezione longitudinale.

3. Constitutive models

3.1. Viscoplastic material model for the ground

A viscoplastic material model is employed in order to describe the behavior of the ground that can lead to squeezing conditions during tunneling.

The plastic material response of the ground is described by means of the Drucker-Prager criterion (Fig. 5a) reading:

$$f_{DP}(\sigma,\zeta_{DP}) = \sqrt{J_2} + \alpha\ I_1 - \zeta_{DP}/\beta \qquad (1)$$

where ζ_{DP} represents the hardening force of the Drucker-Prager criterion. The parameters α and β are computed from the cohesion c and the friction angle φ such that the Drucker-Prager meridian coincides with the compression meridian of the respective Mohr-Coulomb criterion. This yields:

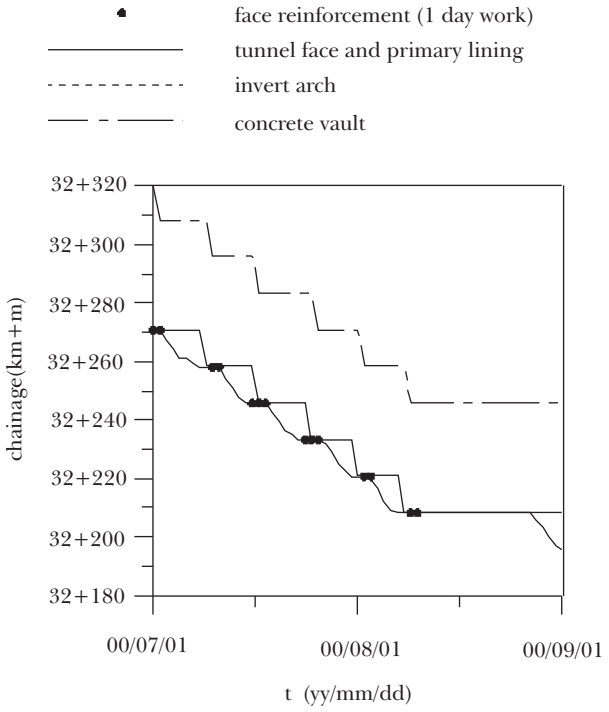

Fig. 4 – Raticosa tunnel, Italy: recording of the construction advance during July and August 2000.
Fig. 4 – La galleria Raticosa, Italia: sequenza delle fasi di scavo durante luglio e agosto 2000.

$$\alpha(\varphi) = \frac{2\sin\varphi}{\sqrt{3}(3-\sin\varphi)},\ \beta(c,\varphi,f_c) = \frac{f_c}{\sqrt{3}c}\frac{3-\sin\varphi}{2\cos\varphi}$$

with $$f_c(c,\varphi) = \frac{2c\cos\varphi}{1-\sin\varphi} \quad (2)$$

denoting the uniaxial compressive strength of the material. An increase in the hardening force ζ_{DP} is disregarded here for sake of simplicity, whit $\zeta_{DP} = f_c$ = constant.

In the tensile loading regime, a tension-cut-off is employed, reading:

$$f_{TC}(\sigma,\zeta_{TC}) = I_1 - \zeta_{TC} \quad (3)$$

with ζ_{TC} representing the hardening force. For the tension-cut-off, an ideally plastic behavior is assumed. Hence, $\zeta_{TC} = f_t$ = constant, where f_t is the uniaxial tensile strength, with $f_t \simeq 0$.

The Drucker-Prager criterion and the tension-cut-off are combined in the context of multi-surface plasticity. The evolution equation for the plastic strain tensor is given by [KOITER, 1969]:

$$\dot{\varepsilon}^p = \dot{\gamma}_{DP}\frac{\partial g_{DP}}{\partial\sigma} + \dot{\gamma}_{TC}\frac{\partial f_{TC}}{\partial\sigma} \quad (4)$$

where $g_{DP}(\sigma) = \sqrt{J_2} + \bar{\alpha} I_1$ represents the plastic potential of the Drucker-Prager criterion. $\bar{\alpha}$ is computed from the dilation angle ψ, with $\bar{\alpha} = 2\sin\psi/\sqrt{3}/(3-\sin\psi)$. In Equation (4), γ_{DP} and γ_{TC} stand for the plastic multipliers of the Drucker-Prager criterion and tension-cut-off, respectively. The extension of the described multi-surface plasticity model towards viscoplasticity follows the law proposed by DUVAUT & LIONS [1972], reading:

$$\dot{\varepsilon}^{vp} = \frac{1}{\tau}C^{-1}(\sigma-\sigma^{\infty}) \text{ and } \dot{\zeta}_{DP} = -\frac{1}{\tau}(\zeta_{DP}-\zeta_{DP}^{\infty}), \quad (5)$$

where $\boldsymbol{C}$ denotes the elastic material tensor. In Equation (5), τ is the relaxation time; σ and ζ_{DP} correspond to the solution for rate-independent elastoplasticity, i.e., to the solution of infinitely slow loading.

3.2. Thermo-chemo-mechanical material model for shotcrete

During the installation of the primary lining, shotcrete is applied onto the newly excavated surfaces of the tunnel. Already at an early age, i.e., during the chemical reaction between cement and water (hydration), the shotcrete is loaded mechanically by the inward moving rock mass.

For the simulation of shotcrete under such loading conditions, a thermo-chemo-mechanical material model was developed at the Vienna University of Technology, see [HELLMICH *et al.*, 2001; SERCOMBE *et al.*, 2000; LACKNER *et al.*, 2002].

Shotcrete is modeled in the framework of chemically reactive porous media [COUSSY, 1995]. The hydration process is described by the degree of hydration which is defined by the mass of formed hydrates, m, related to the mass of formed hydrates at complete hydration, m_∞:

$$\xi = \frac{m}{m_\infty} \quad \text{with } 0 \le \xi \le 1. \quad (6)$$

The thermally-activated nature of the hydration process is accounted for by an Arrhenius-type evolution law for ξ, reading [ULM & COUSSY, 1995]:

$$\dot{\xi} = \tilde{A}(\xi)\exp(-E_a/RT) \quad (7)$$

where $\tilde{A}(\xi)$ represents the normalized chemical affinity which is the driving force of the hydration process. E_a is the activation energy, R is the universal gas constant, with $E_a/R = 4000$ K. T is the temperature in K.

Dissipation phenomena at the microlevel of the material are accounted for by means of internal state variables and energetically conjugated thermodynamics forces, related to the state variables via state equations. The rates of internal state variables are related to the corresponding thermodynamic forces by means of appropriate evolution equations.

The following dissipative phenomena govern the material behavior:

- the chemical reaction between water and cement, i.e., hydration, results in chemical shrinkage strains ε^s, aging elasticity, strength growth (chemo-mechanical couplings), and in the release of heat at hydration (thermo-chemical couplings);
- microcracking of the hydrates leads to plastic strains ε^p. The state of microstructural changes resulting from microcracking is described by the hardening variables $\boldsymbol{\chi}$, as in classical plasticity theory. In the present case, a multi-surface model consisting of a Drucker-Prager loading surface and a tension-cut-off loading surface are employed (Fig. 5);
- stress-induced dislocation-like processes within the hydrates result in flow (or long-term) creep strains ε^f. The state of the respective microstructural changes is described by the viscous flow;
- stress-induced microdiffusion of water in the capillary pores between the hydrates results in viscous (or short term) creep strains ε^v.

During the hydration of shotcrete, new hydrates are formed in a state which is free of microstress [BAŽANT, 1979]. This is reflected by an incremental stress-strain law, reading [SERCOMBE *et al.*, 2000]:

$$\Delta\sigma = C(\xi):\left[\Delta\varepsilon - \Delta\varepsilon^p - \Delta\varepsilon^v - \Delta\varepsilon^f - \Delta\varepsilon^s - \Delta\varepsilon^T\right] \quad (8)$$

where $\Delta\sigma$ represents an increment of the stress tensor, $\boldsymbol{C}$ is the (aging) elastic material tensor and $\Delta\varepsilon^T$ stands for an increment of the thermal strain tensor.

In general, the individual processes, i.e., thermal, chemical and mechanical processes, depend on each other. Such dependencies are referred to as couplings (Fig. 6). E.g., the interaction between the hydration process and the deformations is denoted as chemo-mechanical coupling. The interaction between the deformations and the temperature is accounted for by the thermo-mechanical coupling. Finally, the interaction between the hydration and the temperature is referred to as thermo-chemical coupling.

On the basis of experimental evidence, some couplings have a minor influence on the behavior of shotcrete (Fig. 7). E.g., chemo-mechanical coupling is actually a one-way coupling, with the hydration process influencing the mechanical state of the material through shrinkage strains, aging elasticity, and chemical hardening. On the contrary, mechanical deformations only have little influence on the hydration process. In the same way, the thermo-mechanical coupling is actually a one-way coupling, with temperature changes resulting in temperature strains.

Based on the one-way couplings depicted in Figure 7, both thermal and chemical processes are not influenced by mechanical deformations. This makes it possible to split the numerical analysis into two parts: a thermo-chemical analysis for determining the temperature field and the field of degrees of hydration, and a subsequent mechanical analysis.

The mixture characteristics and the material properties of the considered shotcrete are listed in Table III.

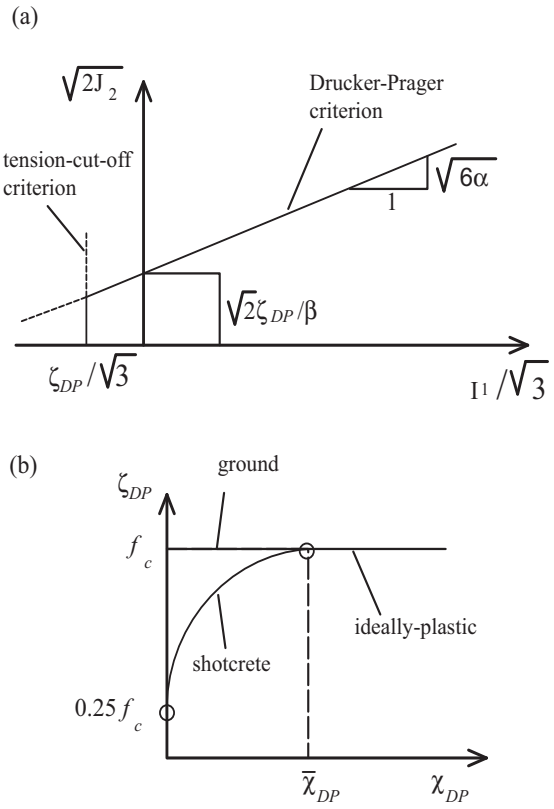

Fig. 5 – Multi-surface plasticity model for ground and shotcrete: (a) yield surfaces and (b) strain-hardening according to the Drucker-Prager criterion.
Fig. 5 – Modello plastico multisuperficie per il terreno ed il calcestruzzo proiettato: (a) superfici di snervamento e (b) legge di incrudimento del criterio di Drucker-Prager.

4. Solution of the thermo-chemical problem

During the hydration of shotcrete, hydration heat l_ξ is released resulting in an increase in the temperature in the shotcrete lining and, hence, in heat conduction into the surrounding ground and heat

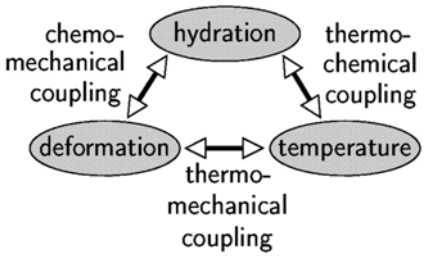

Fig. 6 – Material model for shotcrete: possible couplings between thermal, chemical, and mechanical processes.
Fig. 6 – Modello costitutivo per il calcestruzzo proiettato: possibili accoppiamenti fra i processi termici, chimici e meccanici.

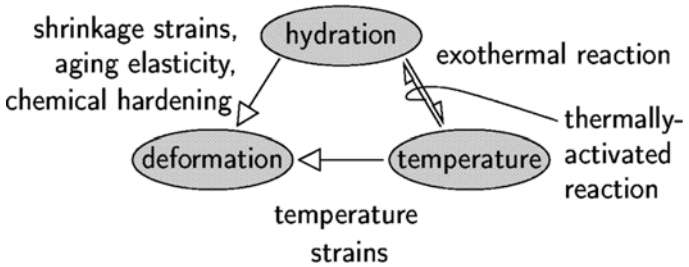

Fig. 7 – Material model for shotcrete: relevant couplings.
Fig. 7 – Modello costitutivo per il calcestruzzo proiettato: accoppiamenti rilevanti.

Tab. III – Mixture characteristic and material properties of the shotcrete considered in the numerical analyses.
Tab. III – Caratteristiche della miscela e proprietà meccaniche del tipo di calcestruzzo proiettato adottato nelle analisi numeriche.

Cement content	c [kg/m^3]	380
Aggregate/cement ratio	a/c [–]	4.79
Water/cement ratio	w/c [–]	0.60
Compressive strength	$f_{c,}$ [MPa]	19.8
$f_c(\xi) = f_{c,\infty}\frac{\xi - \xi_0}{1-\xi_0}$	ξ_0 [–]	0.01
Biaxial compression. strength factor	f_b/f_c [–]	1.16
Young's modulus $E(\xi) = E_\infty\sqrt{\xi}$	E [MPa]	20400
Poisson's ratio	ν [–]	0.2
Characteristic time $\tau_w(\xi) = \xi \cdot \tau_{w,}$	$\tau_{w,}$ [h]	24
Viscous compliance $J^v = J^{v,0}(1-\xi)$	$J^{v,0}$ [1/MPa]	$127 \cdot 10^{-6}$
Softening modulus for flow creep	H [MPa]	$1/7 \cdot 10^6$
Chemical affinity	a_A [1/s]	7.313
	b_A [–]	10.46
$\widetilde{A}(\xi) = a_A\frac{1-\exp(-b_A\xi)}{1+c_A\xi^{d_A}}$	c_A [–]	169.3
	d_A [–]	4.37
Chemical dilation angle	a_s [–]	$-0.405 \cdot 10^{-3}$
$\beta(\xi) = a_s + b_s\xi$	b_s [–]	$0.943 \cdot 10^{-3}$

radiation towards the tunnel cavity. The field equation for the thermo-chemical problem is given by [ULM & COUSSY, 1995]

$$\rho\dot{c}T - l_\xi\dot{\xi} = \mathrm{div}\mathbf{q}, \tag{9}$$

with ρ as the density and c as the heat capacity. $\boldsymbol{q}$ is the heat flow vector. It is related to the temperature via the linear law of Fourier:

$$\boldsymbol{q} = -k \cdot \mathrm{grad}T \tag{10}$$

where k is the thermal conductivity.

4.1. Structural model, boundary conditions, and FE discretization

For determining the temperature profiles in consequence of the hydration process, a 1D axisymmetric FE model is employed (Fig. 8). The respective FE formulation for the solution of the axisymmetric thermo-chemical problem can be found in [LACKNER & MANG, 2002]. The FE model refers to a section perpendicular to the axis of tunnel. It comprises both the shotcrete lining and the surrounding ground. The thickness of the shotcrete lining is set equal to 30 cm. It is discretized with 5 finite elements in the radial direction. The surrounding rock is discretized with 36 finite elements.

At the inner surface of the shotcrete lining, heat radiation from the lining to the tunnel opening is considered. The underlying heat radiation law reads:

$$q = \alpha_R (T - T_\infty) \tag{11}$$

with T standing for the temperature at the inner surface of the lining and T_∞ for the temperature of the air in the tunnel cavity. α_R is the radiation coefficient.

4.2. Material properties and initial temperature

The thermal properties of the shotcrete and the ground employed in the numerical analysis are listed in Table IV.

The initial temperature of the shotcrete lining and the ground are taken to be 20 and 10 °C, respectively. The temperature in the tunnel opening, T_∞, is assumed to be 25 °C.

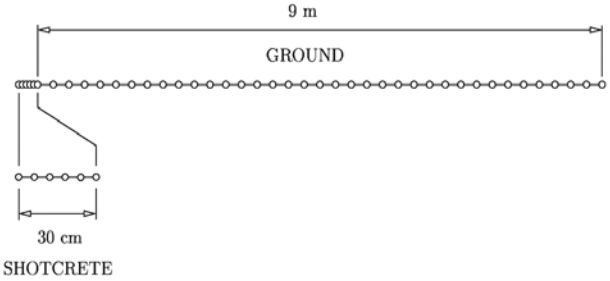

Fig. 8 – Thermo-chemical analysis: 1D axisymmetric FE mesh.
Fig. 8 – Analisi termo-chimica: maglia assialsimmetrica 1D per l'analisi agli elementi finiti.

Tab. IV – Thermo-chemical analysis: material parameters for shotcrete and ground.
Tab. IV – Analisi termo-chimica: parametri adottati per il calcestruzzo proiettato e per il terreno.

SHOTCRETE		
Heat capacity	ρc [kJ/(m^3 K)]	2428
Thermal conductivity	k [kJ/(m h K)]	12.6
Heat of hydration	l_ξ [kJ/m^3]	190000
Radiation coefficient shotcrete-air	α_R [kJ/(m^2 h K)]	40
GROUND		
Heat capacity	ρc [kJ/(m^3 K)]	2300
Thermal conductivity	k [kJ/(m h K)]	7.2

4.3. Presentation of results

Figure 9 shows the evolution of the mean temperature T_m in the shotcrete lining as a function of time. The maximum value of T_m, 32.5 °C, is reached about 18 hours after installation of the lining.

The distribution of the temperature in the shotcrete lining and in the adjacent ground at different time instants is given in Figure 10. Temperature profiles like these serve as input for the following mechanical analysis.

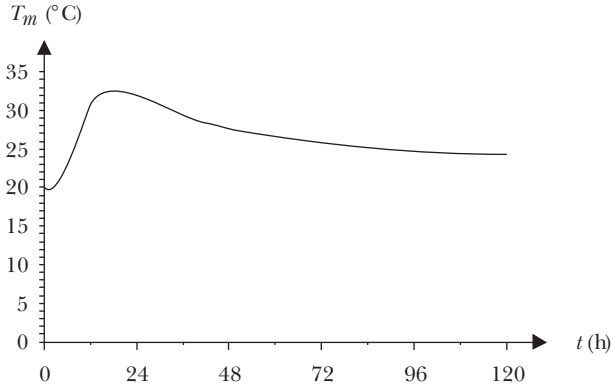

Fig. 9 – Thermo-chemical analysis: mean temperature T_m of the shotcrete lining as a function of time.
Fig. 9 – Analisi termo-chimica: andamento della temperatura media T_m in funzione del tempo del rivestimento in calcestruzzo proiettato.

5. Solution of the mechanical problem: numerical model

5.1. Structural model and FE discretization

The axisymmetric model employed for the solution of the mechanical problem makes it possible to simulate both a continuous excavation of the tunnel with a driving speed of 2.5 m/day, and the construction break during the summer holidays according to the excavation of the Raticosa tunnel during July and August 2000.

As pointed out in [BOLDINI *et al.*, 2003], an excavation length of 10R considered in the structural model, where R is the radius of the tunnel, is sufficient to avoid boundary effects influencing the numerical solution. Accordingly, the length of the structural model was set equal to 20R (Fig. 11b). The excavation starts from the right boundary and is stopped when the tunnel face reaches the center of the model, i.e., after the excavation of 10R of tunnel length. Continuation of the analysis for three weeks without any excavation allows to simulate the situation during summer holidays.

A local coordinate system is introduced. The coordinate r refers to the radial direction, whereas the coordinate z is oriented along the longitudinal direction of the tunnel. $z=0$ refers to the final location of the tunnel face.

A circular tunnel with a radius $R=7$ m is chosen for all numerical analyses (Fig. 11a). After excava-

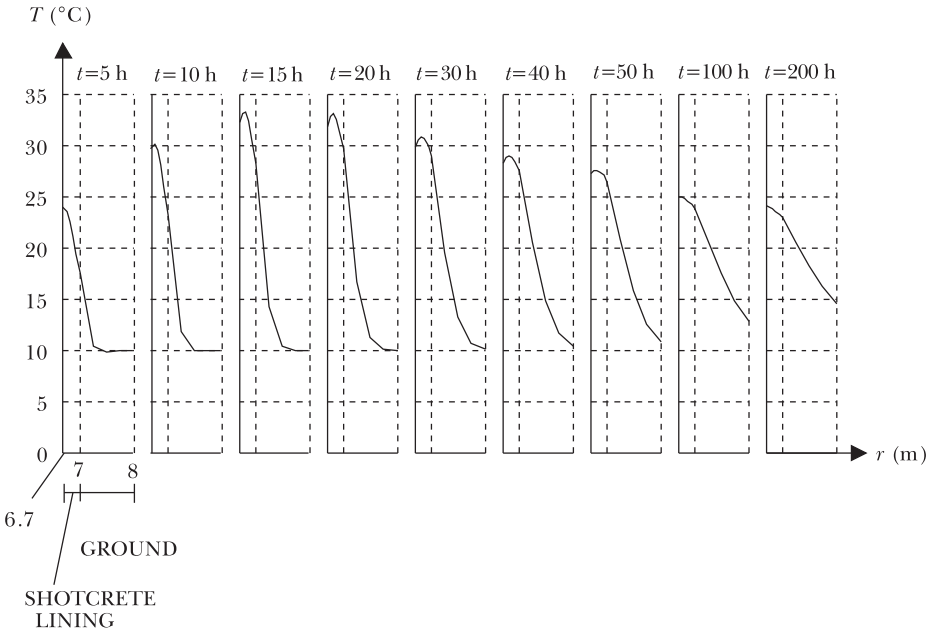

Fig. 10 – Thermo-chemical analysis: distribution of the temperature T in the shotcrete lining and in the ground at different time instants.
Fig. 10 – Analisi termo-chimica: distribuzione della temperatura T nel rivestimento in calcestruzzo proiettato e nel terreno per differenti istanti di tempo.

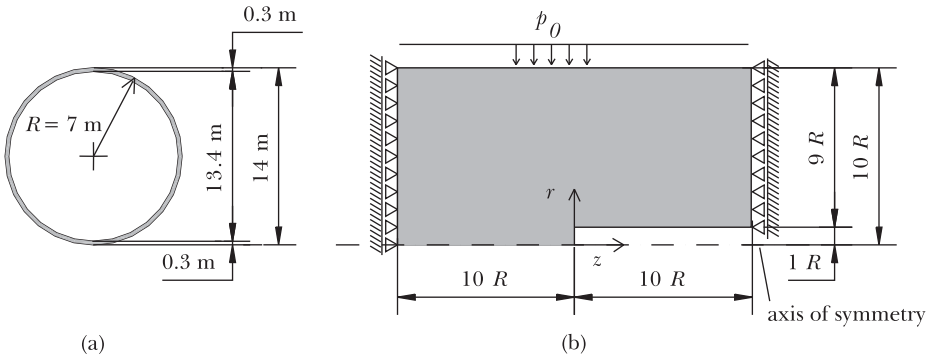

Fig. 11 – Mechanical analysis: (a) cross section of the tunnel and (b) geometric dimensions of the structural model.
Fig. 11 – Analisi meccanica: (a) sezione trasversale della galleria e (b) dimensioni del modello strutturale.

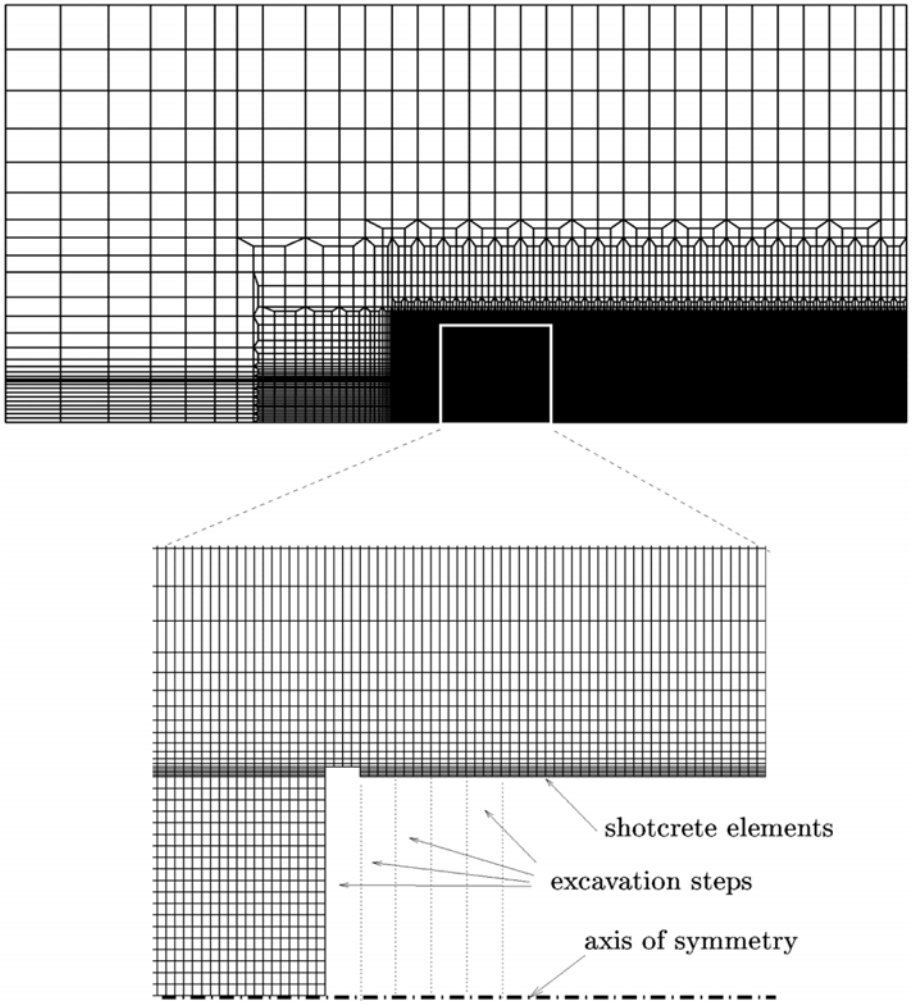

Fig. 12 – Mechanical analysis: FE mesh consisting of 15266 axisymmetric four-node elements.
Fig. 12 – Analisi meccanica: maglia per l'analisi agli elementi finiti costituita da 15266 elementi assialsimmetrici a quattro nodi.

tion, the application of a closed 30 cm-thick shotcrete shell is considered.

Figure 12 shows the FE discretization consisting of 15266 axisymmetric finite elements. Near the tunnel face, the mesh is refined in order to provide better approximations of the rather high stress and strain gradients in this area.

5.2. Excavation scheme

The excavation of the tunnel is simulated by replacing the respective ground elements by cavity elements. The latter are characterized by marginal stiffness. Application of shotcrete is modeled by replacing the respective cavity elements by finite ele-

ments with shotcrete characteristics. Similar to the FE discretization employed for the thermo-chemical analysis, the shotcrete shell is discretized over the thickness by means of five finite elements.

The length of one excavation step and, hence, the length of the unsupported part of the tunnel is set equal to 1 m. This value is in agreement with the excavation step adopted in the Raticosa tunnel during July and August 2000.

Similarly, the excavation rate is set equal to 2.5 m/day. The time assigned to complete 1 m of tunnel is divided into two parts: 2/3 of the time is dedicated to the excavation and the remaining 1/3 to the application of shotcrete. For an excavation rate of 2.5 m/day, 1 m of tunnel is completed in 9.6 hours. Consequently, 2/3·9.6= 6.4 hours are assigned to the excavation process and 1/3·9.6= 3.2 hours to the application of the shotcrete lining.

After the tunnel face has reached its final position at z= 0 m, the excavation is stopped. The analysis, however, is continued for three weeks in order to simulate a typical break period during summer holidays.

5.3 Initial state of stress

Axisymmetric conditions are considered. The tunnel axis is assumed to be horizontal and to coincide with the axis of symmetry. This implies that the initial state of stress that is adopted for the numerical analyses is isotropic. The isotropic stress is set equal to σ_0= 2.8 MPa. This value corresponds to the *in situ* stress conditions of a tunnel at a depth h= 150 m characterized by a ground weight per unit volume γ= 25 kN/m^3 and a lateral pressure coefficient K_0= 0.5.

In the structural model, the initial stress state is introduced by setting the principal stresses equal to 2.8 MPa in all finite elements and by applying a constant pressure p_0 at the top boundary of the model, with p_0= 2.8 MPa (see Fig. 11b).

5.4. Consideration of dowels in the FE model

In the FE model, fiber-glass dowels having a length of 24 m are considered. They are discretized by means of chains consisting of two-node truss elements. The nodes of each truss element are connected to the respective nodes of the ground elements. Accordingly, no slip between the dowels and the ground is considered.

The distance between two subsequent settings of dowels is set equal to 13 m. For an excavation length of 70 m, as considered in the structural model (Fig. 11b), the setting of dowels is simulated at the following positions of the tunnel face: z= 65, 52, 39, 26, 13, and 0 m.

The layout of the face reinforcement considered in the numerical analysis is illustrated in Figure 13 for installation of the dowels at z=0. The location of two consecutive face reinforcements differs by the radial location of the dowels. The radial distance between two corresponding sets of dowels is 35 cm.

In axisymmetric analyses, the dowels, which are set at different locations of the tunnel face, must be shifted towards the axisymmetric plane (Fig. 14). Consequently, each of the dowels shown in Figure 13 represents the total number of dowels having the same distance from the axis of symmetry. A total number of 45 dowels is placed during a single reinforcement step. Accordingly, each of the different dowels of the axisymmetric model represents 4, 7, 6, 11, 10, and 7 real dowels (Fig. 13).

The time assigned to install the dowels at the tunnel face is 3 days, according to the time schedule of the Raticosa tunnel (Fig. 4).

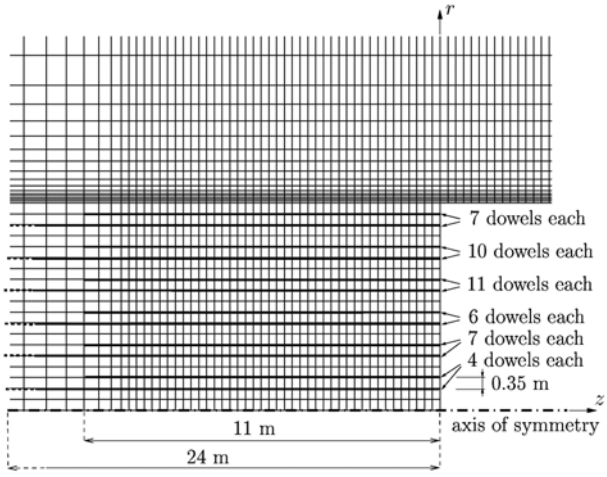

Fig. 13 – Mechanical analysis: location of truss elements representing fiber-glass dowels of 24 m length used for face reinforcement.
Fig. 13 – Analisi meccanica: posizione degli elementi di tipo asta rappresentanti le barre in vetroresina di 24 m utilizzate per il rinforzo del fronte.

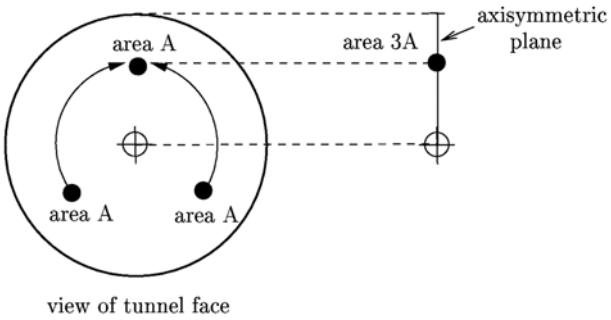

Fig. 14 – Mechanical analysis: example of shifting three dowels towards the axisymmetric plane.
Fig. 14 – Analisi meccanica: esempio di spostamento di tre barre verso il piano assialsimmetrico.

For the simulation of the mechanical behavior of the dowels, a linear elastic – ideally plastic material model is employed. The mechanical properties of the fiber-glass dowels used in the numerical analyses are given in Table V.

6. Solution of the mechanical problem: presentation of results

6.1. Analyses performed

The focus of the analyses performed in this study is on investigating the behavior of tunnels excavated in squeezing ground conditions. For this purpose, the ground properties were chosen in such a way as to match conditions indicating a high squeezing potential, with $f_c/\sigma_0 < 0.2$. Four different types of ground were considered, characterized by the following values for ground cohesion: 10 (ground type A), 50 (ground type B), 100 (ground type C), and 150 kPa (ground type D). The remaining material parameters were the same for all ground types and their values are reported in Table VI.

In order to assess the effect of the shotcrete lining and of the fiber-glass dowels on the static conditions of the tunnel, four different analyses were performed for each ground-type condition:

1: in the first analysis, neither the shotcrete lining nor the fiber-glass dowels were considered. In this analysis the behavior of the unlined tunnel is investigated;
2: the installation of shotcrete is considered in the second analysis;
3: both the shotcrete lining and the reinforcement of the tunnel face by means of fiber-glass dowels are considered in the third analysis. The reinforcement density is set equal to 0.29 dowels/(m^2 tunnel face);
4: finally, the fiber-glass dowel density is increased to 0.58 dowels/(m^2 tunnel face).

The synopsis of the full set of performed analyses is given in Table VII.

6.2. Influence of the support

In this subsection, the influence of the different support means (shotcrete primary lining, face reinforcements by fiber-glass dowels) is investigated for ground type B (cohesion c = 50 kPa).

Figure 15 shows the longitudinal deformation u_z/R of the ground ahead the tunnel face (z <0) at r = 0, obtained at time instants (a) t = 1032 h and (b) t = 1608 h. At the time instant t = 1032 h, the tunnel face has reached its final position at z = 0 for a driving speed of 2.5 m/days and five excavation stops of three days each for the installation of the face reinforcement ($t = 70/2.5 + 5 \cdot 3 = 43$ days = 1032 hours). In order to permit comparison between the different analyses, the same excavation stops were considered in analyses B1 and B2, even though no setting of fiber-glass dowels is considered. Between the time instants t = 1032 h and t = 1608 h, the position of the tunnel face remains unchanged in the numerical analyses, thereby making it possible to simulate a three-week construction break due to the summer holidays or to an unexpected stop of advancement.

Analysis B1 gives the highest value for u_z/R, with u_z/R = 10% at the face after the three-week break, indicating the probable collapse of the tunnel. The influence of the primary lining (analysis B2) is remarkable (even ahead the tunnel face), reducing u_z/R to almost one half for both steady-state excavation (Fig. 15a) and temporary stops (Fig. 15b). The influence of the face reinforcement is not considerable at the time instant t = 1032 h. On the contrary, the longitudinal displacements of the

Tab. V – Mechanical analysis: mechanical properties of the fiber-glass dowels.
Tab. V – Analisi meccanica: proprietà meccaniche adottate per le barre in vetroresina.

Young's modulus	E [MPa]	15000
Poisson's ratio	ν [–]	0.3
Yield strength	f_y [MPa]	900

Tab. VI – Mechanical analysis:. mechanical properties of the ground.
Tab. VI – Analisi meccanica: proprietà meccaniche adottate per il terreno.

Friction angle	φ [-]	18°
Dilation angle	ψ [-]	1.8°
Young's modulus	E [MPa]	500
Poisson's ratio	ν [-]	0.3
Relaxation time	τ [h]	0.5

Tab. VII – Mechanical analysis: synopsis of the performed analyses.
Tab. VII – Analisi meccanica: quadro riassuntivo delle analisi numeriche eseguite.

Cohesion c [kPa]:	10	50	100	150
Squeezing potential f_c/σ_0:	0.01	0.05	0.10	0.15
Unlined tunnel	A1	B1	C1	D1
Only shotcrete	A2	B2	C2	D2
Shotcrete + 0.29 dowels/m^2	A3	B3	C3	D3
Shotcrete + 0.58 dowels/m^2	A4	B4	C4	D4

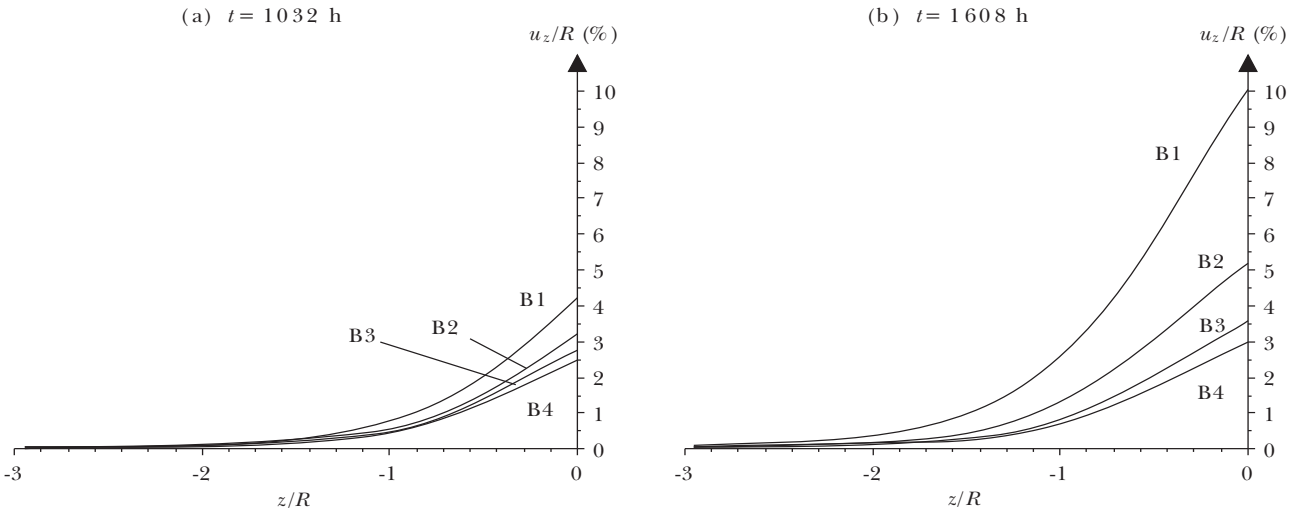

Fig. 15 – Mechanical analysis: longitudinal deformation u_z/R (%) at $r = 0$ obtained at time instants (a) $t = 1032$ h and (b) $t = 1608$ h for the analyses B1, B2, B3, and B4.
Fig. 15 – Analisi meccanica: deformazione longitudinale u_z/R (%) in corrispondenza di $r = 0$ ottenuta agli istanti di tempo (a) $t = 1032$ h e (b) $t = 1608$ h nelle analisi B1, B2, B3, e B4.

ground are appreciably reduced by the fiber-glass dowels after the stop of the excavation, allowing the tunnel face to remain stable. Doubling the dowel density (analysis B4) results in a reduction of u_z/R of 0.5% as compared to analysis B3.

The loading of the reinforcement system is given in Figure 16 for analysis B3 in terms of the average stress in the fiber glass dowels σ_{dm}:

$$\sigma_{dm} = \frac{1}{n_d} \sum_{i=1}^{n_d} \sigma_{d,i} \qquad (12)$$

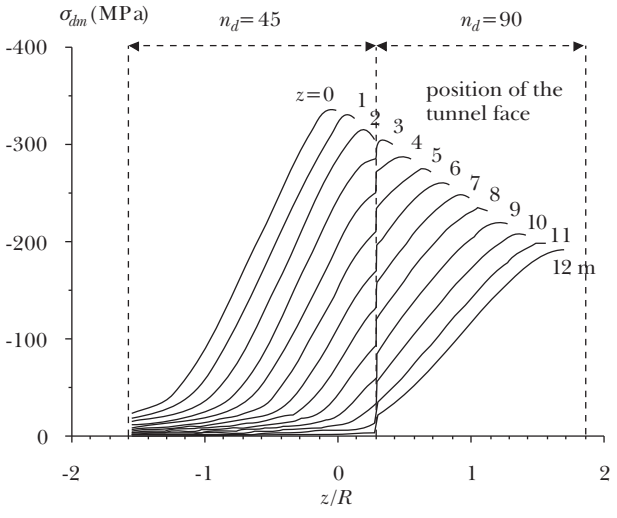

Fig. 16 – Mechanical analysis: average stress σ_{dm} in the fiber-glass dowels during the excavation from $z = 13$ m to $z = 0$ for the analysis B3 for different position of the tunnel face $z = 12$, 11, ...0 m (n_d = number of dowels).
Fig. 16 – Analisi meccanica: sollecitazione media σ_{dm} nelle barre in vetroresina durante lo scavo da $z = 13$ m a $z = 0$ ottenuta nell'analisi B3 in corrispondenza di differenti posizioni del fronte $z = 12$, 11, ...0 m (n_d = numero delle barre).

where $\sigma_{d,i}$ is the stress in the i-th dowel. n_d represents the number of dowels at the considered cross section of the tunnel. In the area of overlapping dowels (see Fig. 13), $n_d = 90$. Otherwise, $n_d = 45$. Figure 16 shows the distribution of σ_{dm} during tunnel excavation from $z = 13$ m to $z = 0$. A new set of fiber-glass dowels is installed at $z = 13$ m, whereas the previous one (installed at $z = 26$ m) reaches to $z = 2$ m. Hence, between $z = 13$ m and $z = 2$ m, $n_d = 90$. In the course of the excavation, the length of the dowels installed at $z = 26$ and $z = 13$ m continuously decreases, resulting in an increase in the average stress. At $z = 2$ m, one set of dowels ends, explaining the jumps in the distribution of σ_{dm}. For all excavation steps plotted in Figure 16, significant loading of the dowels is observed only for a distance ahead of the face equal to one tunnel radius R.

Figure 17 shows the stress σ_d in the set of fiber-glass dowels located at $r = 1.05$ m from the tunnel axis (see Fig. 13) obtained at time instants $t = 1032$ h and $t = 1608$ h. Even though the face is reinforced with a new set of fiber-glass dowels before the excavation break of three weeks, resulting in a total number of 90 dowels installed ahead of the tunnel face, the continued of stress release in the ground results in a significant increase of σ_d.

Figure 18 shows the radial deformation u_r/R of the tunnel wall ($r = R$) as a function of the distance from the tunnel face z/R, obtained at time instants (a) $t = 1032$ h and (b) $t = 1608$ h. For the analysis considering the application of shotcrete, a saw-toothed shape of u_r/R is observed. Each saw-tooth refers to one excavation step of 1 m. The change in u_r within one saw-tooth indicates the variation of displacement and loading within 1 m of the tunnel.

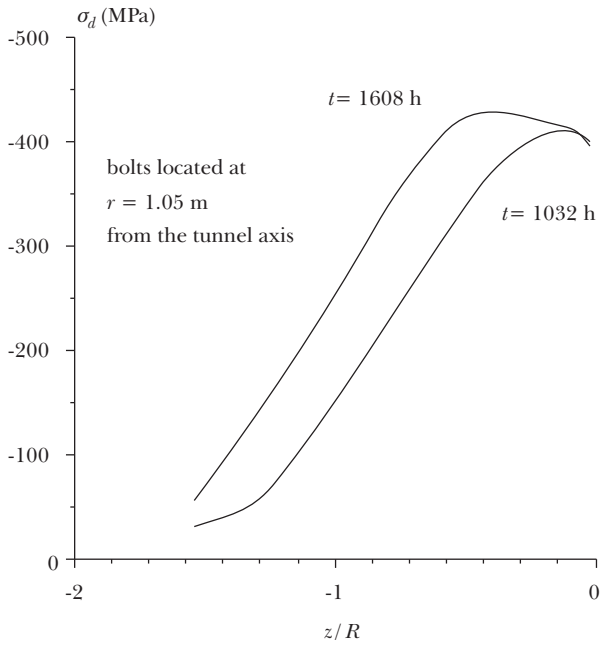

Fig. 17 – Mechanical analysis: stress σ_d in the fiber-glass dowels located at $r = 1.05$ m from the tunnel axis obtained at time instants $t = 1032$ h and $t = 1608$ h.
Fig. 17 – Analisi meccanica: distribuzione della sollecitazione σ_d nelle barre in vetroresina posizionate ad una distanza $r = 1.05$ m dall'asse della galleria ottenuta agli istanti di tempo $t = 1032$ h e $t = 1608$ h.

The installation of the shotcrete lining (analysis B2) led to a huge reduction in the radial deformations with respect to the result obtained for the unlined tunnel (analysis B1). For the latter, the collapse of the tunnel is likely to occur within a short distance from the tunnel face. Almost identical distributions for the radial deformations u_r/R are obtained for analyses B3 and B4 for $z/R>0$, at both time instants $t = 1032$ h and $t = 1608$ h, indicating a negligible influence of the face reinforcement on the convergence of the tunnel. Some differences are visible for $z/R<0$, where the dowels result in a reduction of radial deformations proportional to the reinforcement density. The effect of the excavation break is concentrated near the tunnel face (Fig. 18b), where the relatively high compliance of the young shotcrete, for $z/R>0$, results in an increase of u_r/R.

For analyses B2, B3, and B4, a continuous slight increase of radial deformations is observed. As pointed out in Boldini *et al.* [2003], this increase is a consequence of chemical shrinkage of shotcrete. At the locations of the tunnel corresponding to the installation of the face reinforcement, a localized increase in the radial deformation u_r/R was obtained in all the analyses. This increase is explained by the creep of the ground during the three-days break considered in the analyses to simulate the installation of the face reinforcement.

The distribution of the hoop force n_φ in the shotcrete lining (normalized by the maximum compressive axial force in the shotcrete lining $n = f_c \cdot h = 19.8 \cdot 0.3 = 5.94$ MN/m) is depicted in Figure 19 for time instants (a) $t = 1032$ h and (b) $t = 1608$ h. The average hoop force in the lining is very close to the maximum compressive strength of the shotcrete material, resulting from the severe squeezing conditions simulated in the numerical analyses. With the three-day excavation break for the installation of the face reinforcement, creep of shotcrete results in a slight reduction of the compressive loading. Thereafter, the increase of stiffness during the three-day break leads to a sharp increase in loading after continuation of the excavation. There are no significant differences between the results obtained in analyses B2, B3, and

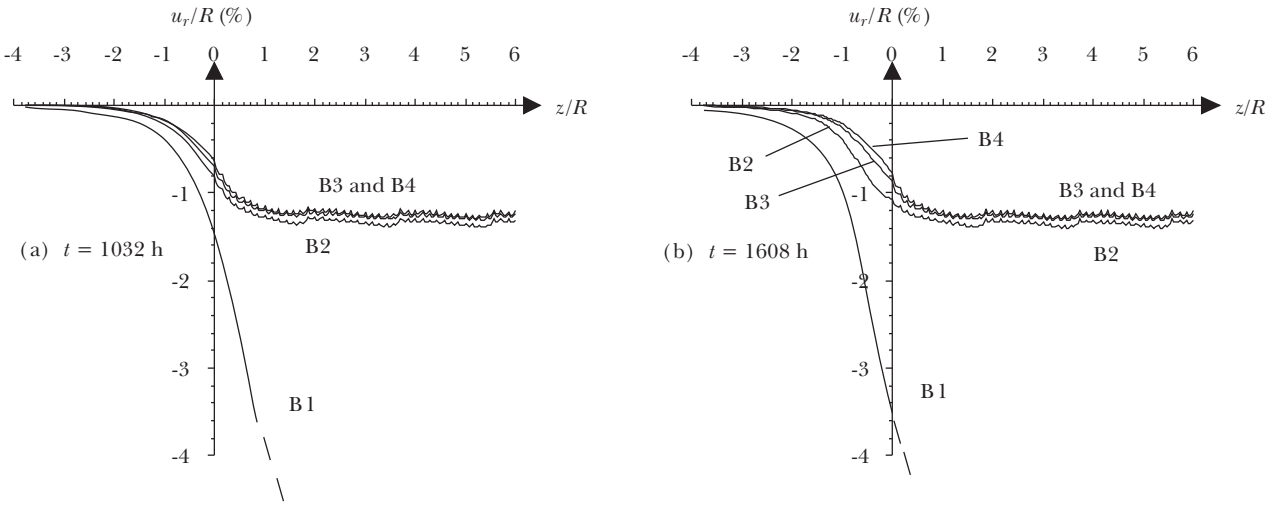

Fig. 18 – Mechanical analysis: radial deformation u_r/R (%) at $r = R$ obtained at time instants (a) $t = 1032$ h and (b) $t = 1608$ h for the analyses B1, B2, B3, and B4.
Fig. 18 – Analisi meccanica: deformazione radiale u_r/R (%) in corrispondenza di $r = R$ attenuta agli istanti di tempo (a) $t = 1032$ h e (b) $t = 1608$ h nelle analisi B1, B2, B3, and B4.

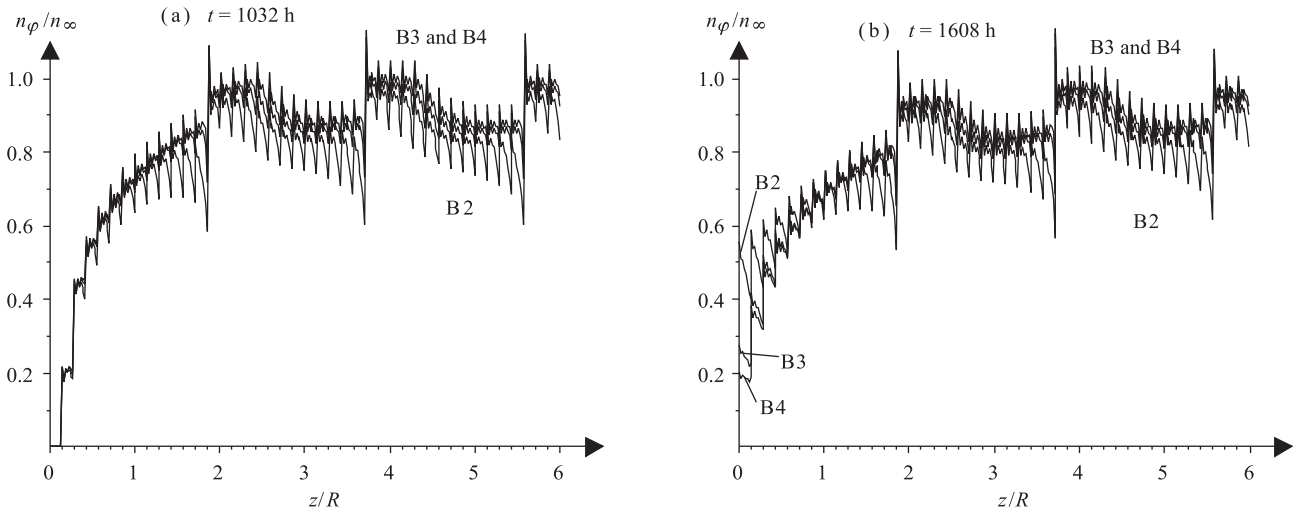

Fig. 19 – Mechanical analysis: distribution of compressive hoop force n_φ/n in the shotcrete lining obtained at time instants (a) t = 1032 h and (b) t = 1608 h for the analyses B2, B3, and B4 ($n = f_{c,} \cdot h = 19.8 \cdot 0.3 = 5.94$ MN/m).
Fig. 19 – Analisi meccanica: distribuzione della forza di compressione circonferenziale n_φ/n nel rivestimento in calcestruzzo proiettato ottenuta agli istanti di tempo (a) t = 1032 h e (b) t = 1608 h nelle analisi B2, B3 e B4 ($n = f_{c,} \cdot h = 19.8 \cdot 0.3 = 5.94$ MN/m).

B4 at time instant t = 1032 h, although the face reinforcement leads to a small increase in the compressive force in the shotcrete lining in analyses B3 and B4 (Fig. 19a). After the three-week excavation break, the plotted distributions are almost unchanged for $z/R > 1$ while a significant increase of n_φ/n is observed near the tunnel face. This increase of the hoop force near the tunnel face is considerably influenced by the density of the face reinforcement: the smaller the dowel density, the greater the relaxation of the ground during the excavation break and the greater the load acting on the shotcrete lining (Fig. 19b).

Figure 20 shows the distribution of the longitudinal force n_z in the shotcrete lining (normalized by the maximum compressive axial force n), for time instants (a) t = 1032 h and (b) t = 1608 h. According to [BOLDINI *et al.*, 2003], the loading of the lining in the longitudinal direction has four reasons: close to the tunnel face, (a) excavation-induced bending of the ground-shotcrete compound structure results in compressive loading which is further increased by (b) the compressive hoop force via Poisson's effect; the compressive loading is reduced by (c) chemical shrinkage and (d) deformations in the longitudinal direction in consequence of the excavation. Analysis B4 gives a higher value of the compressive longitudinal force, which is mainly associated with the more pronounced excavation-induced bending of the shotcrete lining and the higher compressive hoop force via Poisson's effect. The stress release in the ground at the tunnel face during the three-week break results in a sharp increase in the compressive

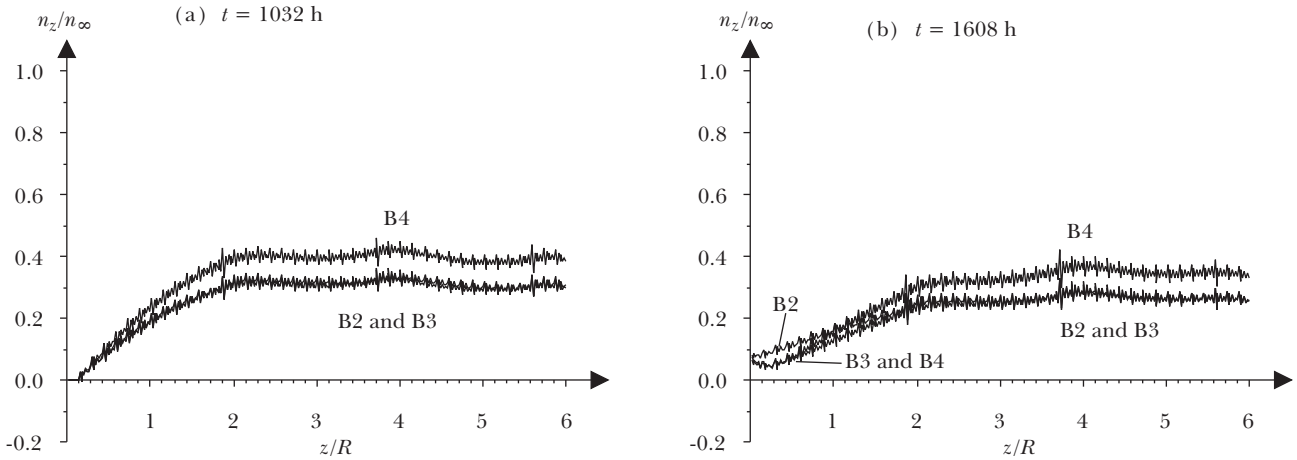

Fig. 20 – Mechanical analysis: distribution of compressive longitudinal force n_z/n in the shotcrete lining obtained at time instants (a) t = 1032 h and (b) t = 1608 h for the analyses B2, B3, and B4 ($n = f_{c,} \cdot h = 19.8 \cdot 0.3 = 5.94$ MN/m).
Fig. 20 – Analisi meccanica: distribuzione della forza di compressione longitudinale n_z/n nel rivestimento in calcestruzzo proiettato ottenuta agli istanti di tempo (a) t = 1032 h e (b) t = 1608 h nelle analisi B2, B3 e B4 ($n = f_{c,} \cdot h = 19.8 \cdot 0.3 = 5.94$ MN/m).

longitudinal force in the final shotcrete segment installed at $0 \leq z \leq 1$ m, which is more significant for analysis B2, where no face reinforcement is considered (see Fig. 20b). For $z/R < 2$, chemical shrinkage of the shotcrete results in a reduction in compressive loading in the longitudinal direction.

6.3. Influence of ground cohesion

The influence of ground cohesion (i.e., of the ratio f_c/σ_0) and of the density of the face reinforcement on the static conditions of the tunnel is shown in Figure 21. Column (a) refers to the numerical results obtained at time instant $t = 1032$ h while column (b) reports the results obtained at $t = 1608$ h, after having stopped the face advance for three weeks.

Face reinforcement turns out to be very effective in reducing longitudinal deformations u_z/R at the tunnel face ($r = 0$ and $z = 0$) in very high squeezing conditions ($f_c/\sigma_0 = 0.01$ and 0.05), especially when relaxation of the ground is allowed during the excavation stop. In this sense, the ground viscosity is found to improve face stability during tunneling in squeezing conditions. The reduction of the face deformation by face reinforcement becomes less pronounced for increasing values of f_c/σ_0.

The more bolts are installed during face reinforcement, the lower the average stress in the dowels (the maximum value obtained at $z/R = -0.05$ is reported in Fig. 21). The average stress in the dowels is reduced almost linearly as the ground cohesion increases, even at time instant $t = 1608$ h.

The radial deformations u_r/R of the tunnel wall at the face ($z = 0$ and $r/R = 1$) reflect the same influence of ground cohesion and reinforcement density as already observed for the longitudinal deformations. Radial deformations are much smaller than the longitudinal deformations, thanks to the immediate support of the shotcrete lining which is applied up to the tunnel face every meter of excavation.

Finally, the normalized hoop force in the shotcrete lining at a great distance from the face ($z/R = 5.01$) is illustrated in Figure 21. The increase in the final load on the lining as the dowel density increases results from the reduction of the early stress relaxation of the ground surrounding the face by means of face reinforcement. No substantial modifications are induced in the shotcrete lining during the three-week stop of tunnel excavation.

7. Summary and conclusions

In this paper, the ground-support interaction in tunneling, characterized by full-face excavation, reinforcement by fiber-glass dowels, and the immediate support with a primary lining of shotcrete, was investigated numerically. The construction scheme adopted in the numerical analyses was based on the design characteristics and the performance of the recently-built Raticosa tunnel, Italy.

A viscoplastic material model was adopted to simulate the squeezing behavior of the ground. Moreover, different values of cohesion were considered in order to account for different squeezing potentials during tunnel excavation.

By employing a thermo-chemo-mechanical material model for shotcrete, two separate analyses were performed. First, the thermo-chemical problem related to the hydration process of shotcrete was solved. Then, the mechanical problem was solved thus providing insight into the state of stress and deformation in the ground, the shotcrete lining, and the fiber-glass dowels. Four different situations, characterized by (1) the unlined and (2) the lined tunnel without face reinforcement and, finally, the lined tunnel with (3) 0.29 dowels/(m^2 tunnel face) and (4) 0.58 dowels/(m^2 tunnel face), were considered.

The following conclusions can be drawn from the obtained numerical results:

- the primary lining of shotcrete was found to play an essential role in assuring the stability of the tunnel in squeezing ground conditions by reducing both the longitudinal and the radial displacements in the ground;
- the reduction of face deformation by the fiber-glass dowels was remarkable in poor ground conditions; it was essential during the excavation stops, avoiding the collapse of the tunnel face by the creeping ground;
- the reduction of ground deformations during tunneling by face reinforcement results in a slight increase of the final load in the shotcrete lining.

The investigation of the complex interaction between the ground, the shotcrete lining, and the face reinforcement by fiber-glass dowels still requires additional parametric analyses, focusing on the main parameters influencing the ground-shotcrete interactions in NATM tunneling, such as (a) the ratio between the characteristic time of ground deformation (given by both the ground viscosity and the tunnel excavation rate) and the characteristic time of the shotcrete hydration process and (b) the delay between the excavation and the installation of the shotcrete support [see BOLDINI *et al*,. 2005]. Moreover, the modeling of the face reinforcement should account for the relative stiffness between the ground and the dowels, as proposed in WONG *et al.* [2002]. All these features are topics of the ongoing research activity.

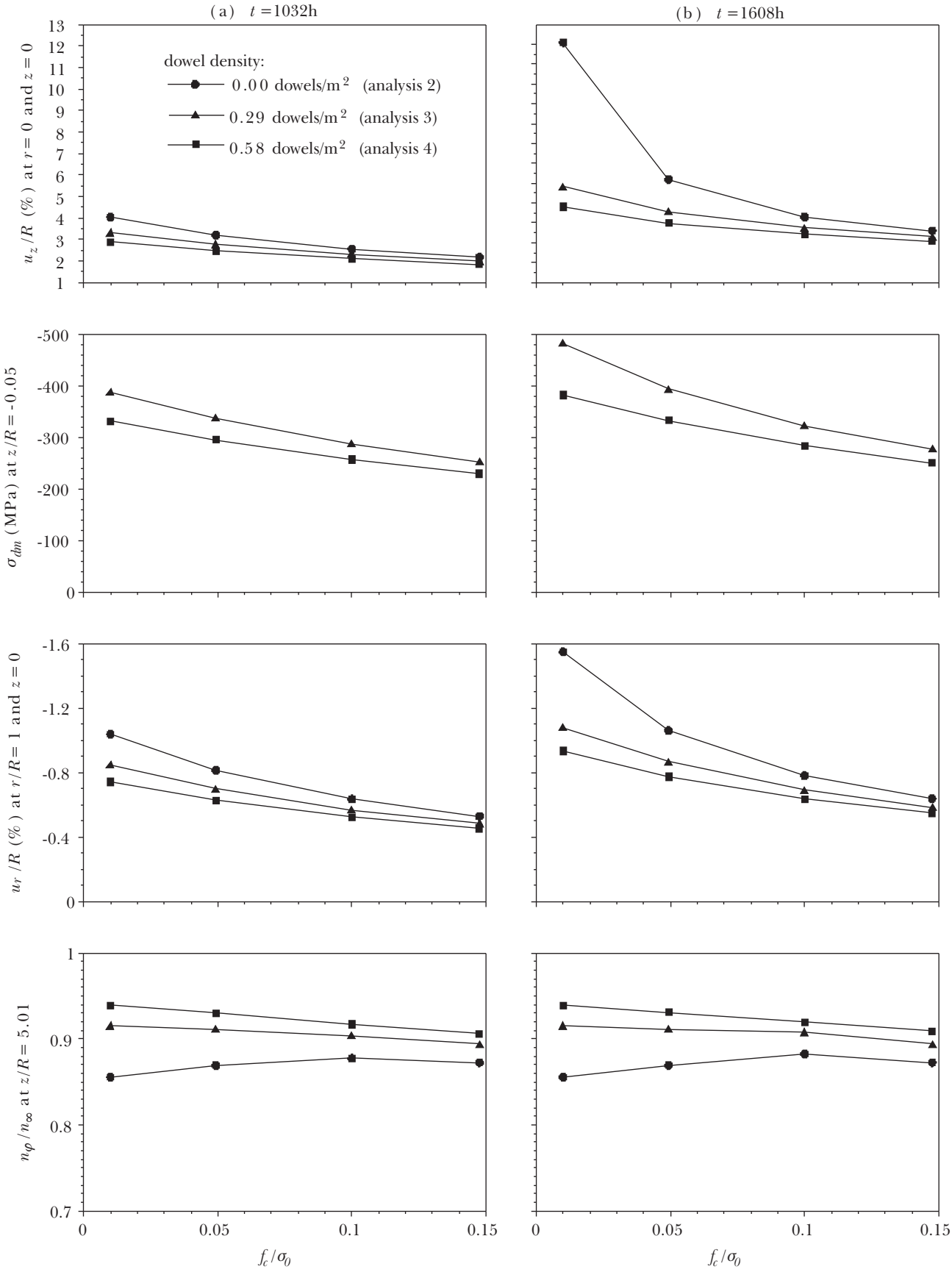

Fig. 21 – Synopsis of the numerical results accounting for the influence of ground cohesion and the density of face reinforcement.

Fig. 21 – Riepilogo dei risultati delle analisi numeriche volte alla valutazione dell'influenza della coesione del terreno e della densità di rinforzo del fronte di scavo.

References

BAŽANT Z. (1979) – *Thermodynamics of solidifying or melting viscoelastic material*. Journal of the Engineering Mechanics Division (ASCE) 105(6), pp. 933-952.

BOLDINI D., LACKNER R., MANG H.A. (2003) – *Elucidation of ground-lining interaction in NATM tunneling accounting for chemo-mechanical couplings in shotcrete behavior*. In C. Viggiani (Ed.), Constitutive Modelling and Analysis of Boundary Value Problems in Geotechnical Engineering, pp. 461-487; Proc. Workshop, Napoli, 22-24 April 2003. Benevento, Hevelius.

BOLDINI D., LACKNER R., MANG H.A. (2004) – *Ground-shotcrete interaction of NATM tunnels with high overburden*. Journal of Geotechnical and Geoenvironmental Engineering (ASCE), In print.

BOLDINI D. GRAZIANI A., RIBACCHI R. (2005) – *Raticosa tunnel, Italy: characterization of tectonized clay-shale and analysis of monitoring data and face stability*. Soils and Foundations, 44, 1, pp. 59-71.

COUSSY O. (1995) – *Mechanics of Porous Continua*. Chichester, Wiley.

DIAS D., KASTNER R., SUBRIN D., WONG H., DUBOIS P. (1998) – *Behavior of a tunnel face reinforced by bolts: comparison between analytical-numerical models*. In A. Evangelista & L. Picarelli (Eds.), *The Geotechnics of Hard Soils – Soft Rocks*, pp. 961-972, Proc. Int. Symp., Napoli, 12-14 October 1998. Rotterdam, Balkema.

DUVAUT G., LIONS J. (1972) – *Les Inéquations en Méchanique et en Physique*. Paris, Dunot.

HELLMICH C., LECHNER M., LACKNER R., MACHT J., MANG H.A. (2001) – *Creep in shotcrete tunnel shells*. In S. Murakami & N. Ohno (Eds.), *Creep in Structures 2000*, pp. 217-229; Proc. Intern. Symp., Nagoya. Dordrecht, Kluwer Academic Publishers.

INTERNATIONAL SOCIETY FOR ROCK MECHANICS (ISRM) (1994) – *Comments and recommendations on design and analysis procedures for structures in argillaceous swelling rock*. International Journal of Rock Mechanics and Mining Sciences & Geomechanical Abstracts, 31, 5, pp. 535-546.

JASSIONNESSE C., DUBOIS P., SAITTA A. (1996) – *Tunnel face reinforcement by bolting: soil bolts homogenization, strain approach*. In R. Mair & N. Taylor (Eds.), *Geotechnical Aspects of Underground Construction in Soft Ground*, pp. 373-378, Proc. Int. Symp., London. Rotterdam, Balkema.

KOITER W. (1969) – *General theorems for elastic-plastic solids*. Amsterdam, North-Holland Publishing Company.

KOVARI K., AMBERG F., EHRBAR H. (2000) – *Mastering of squeezing rock in the Gotthard Base tunnel*. World Tunnelling, 13, 5, pp. 234-238.

LACKNER R., HELLMICH C., MANG H.A. (2002) – *Constitutive modeling of cementitious materials in the framework of chemoplasticity*. International Journal for Numerical Methods in Engineering, 53, 10, pp. 2357-2388.

LACKNER R., MANG H.A. (2002) – *Modeling of early-age fracture of shotcrete: application to tunneling*. In B. Karihaloo (Ed.), *Analytical and Computational Fracture Mechanics of Non-homogeneous Materials*, pp. 197-210, Proc. of the IUTAM Symp., Cardiff, Dordrecht Kluwer Academic Publishers.

LUNARDI P., FOCARACCI A. (1999) – *The Bologna to Florence high speed railway line: progress for underground*. In ALTEN *et al*. (Eds.), *Challenges for the 21st century*, pp. 585-593, Proc. Int. Conf., Oslo.

LUNARDI P. (2000) – *The design and construction of tunnels using the approach based on the analysis of controlled deformation in rocks and soils*. Tunnels & Tunnelling International, 5, pp. 3-29.

NG C.W.W., LEE G.T.K. (2002) – *A three-dimensional parametric study of the use of soil nails for stabilizing tunnel faces*. Computer and Geotechnics, 29, pp. 673-697.

PEILA D. (1994) – *A theoretical study of reinforcement influence on the stability of a tunnel face*. Geotechnical and Geological Engineering, 12, pp. 145-168.

PEILA D., ORESTE P.P., PELIZZA S., POMA A. (1996) – *Study of the influence of sub-horizontal fiber-glass pipes on the stability of a tunnel face*. In L. Ozdemir (Ed.), *North American Tunneling '96*, pp. 425-432, Proc. Int. Symp., Washington D.C.. Rotterdam, Balkema.

SERCOMBE J., HELLMICH C., ULM F.J., MANG H.A. (2000) – *Modeling of early-age creep of shotcrete. I: model and model parameters*. Journal of Engineering Mechanics (ASCE), 126, 3, pp. 284-291.

SCHUBERT W., MORITZ B., SELLNER P. (2000) – *Tunnelling methods for squeezing ground*. Rivista Italiana di Geotecnica, 34, 1, pp. 16-21.

ULM F.J., COUSSY O. (1995) – *Modeling of thermochemo-mechanical couplings of concrete at early ages*. Journal of Engineering Mechanics (ASCE), 121, 7, pp. 785-794.

WONG H., SUBRIN D., DIAS D. (2000) – *Extrusion movements of a tunnel head reinforced by finite length bolts – a closed-form solution using homogenization approach*. International Journal for Numerical and Analytical Methods in Geomechanics, 24, pp. 533-565.

YOO C. (2002) – *Finite-element analysis of tunnel face reinforced by longitudinal pipes*. Computers and Geotechnics, 29, pp. 73-94.

YOO C., SHIN H. (1999) – *Behavior of a tunnel face pre-reinforced with sub-horizontal pipes*. In KUSAKABE *et al*. (Eds.), *Geotechnical Aspects of Underground Construction in Soft Ground*, pp. 441-446, Proc. Int. Symp., Tokyo. Rotterdam, Balkema.

Influenza del rinforzo del fronte e del supporto offerto dal calcestruzzo proiettato sulle condizioni statiche di gallerie profonde: uno studio termo-chimico-meccanico

Sommario

Negli ultimi anni, la combinazione del calcestruzzo proiettato quale rivestimento di prima fase e del rinforzo del fronte mediante barre in vetroresina è stata utilizzata con successo per lo scavo di gallerie in condizioni spingenti (ad esempio in rocce tenere sotto elevati carichi litostatici). In questo articolo sono presentati i risultati di analisi numeriche assialsimmetriche in cui sono stati modellati l'applicazione di un rivestimento in calcestruzzo proiettato e il rinforzo del fronte di scavo mediante barre in vetroresina durante lo scavo di una galleria. Le proprietà geometriche e meccaniche dei sistemi di supporto, così come la sequenza delle fasi di scavo, di applicazione del calcestruzzo proiettato, e del rinforzo del fronte sono stati selezionati facendo riferimento alle caratteristiche di progetto e alle modalità di scavo di una galleria italiana di recente realizzazione (la galleria Raticosa). Lo studio numerico si è concentrato sull'analisi del comportamento di gallerie profonde in condizioni di potenziale spingente da medio ad alto. Di conseguenza, è stato scelto un modello costitutivo viscoplastico per descrivere il comportamento meccanico del terreno. Il comportamento del calcestruzzo proiettato è descritto nell'ambito della teoria accoppiata termo-chimico-meccanica. I risultati ottenuti fanno luce su aspetti legati all'interazione terreno-calcestruzzo proiettato, all'effetto del rinforzo del fronte mediante barre in vetroresina e allo stato di sforzo nello stesso rivestimento in calcestruzzo proiettato. Inoltre, la variazione delle proprietà del terreno e della densità del rinforzo del fronte hanno permesso una valutazione del livello di sollecitazione e quindi dell'efficacia dei sistemi di supporto adottati per differenti condizioni geotecniche.